Supporting Information

Evolutionary expansion of the amidohydrolase superfamily in bacteria in response to synthetic compounds: the molinate and diuron hydrolases.

Elena Sugrue[†], *Nicholas J Fraser*[†], *Davis H Hopkins*[†], *Paul D Carr*[†], *Jeevan L Khurana*[‡], *John G Oakeshott*[‡], *Colin Scott*[‡], *Colin J Jackson*[#, †, ‡]

[†]Research School of Chemistry, Australian National University, Canberra, ACT, Australia; [‡]CSIRO Entomology, Canberra, ACT, Australia

#Corresponding author. Email: colin.jackson@anu.edu.au

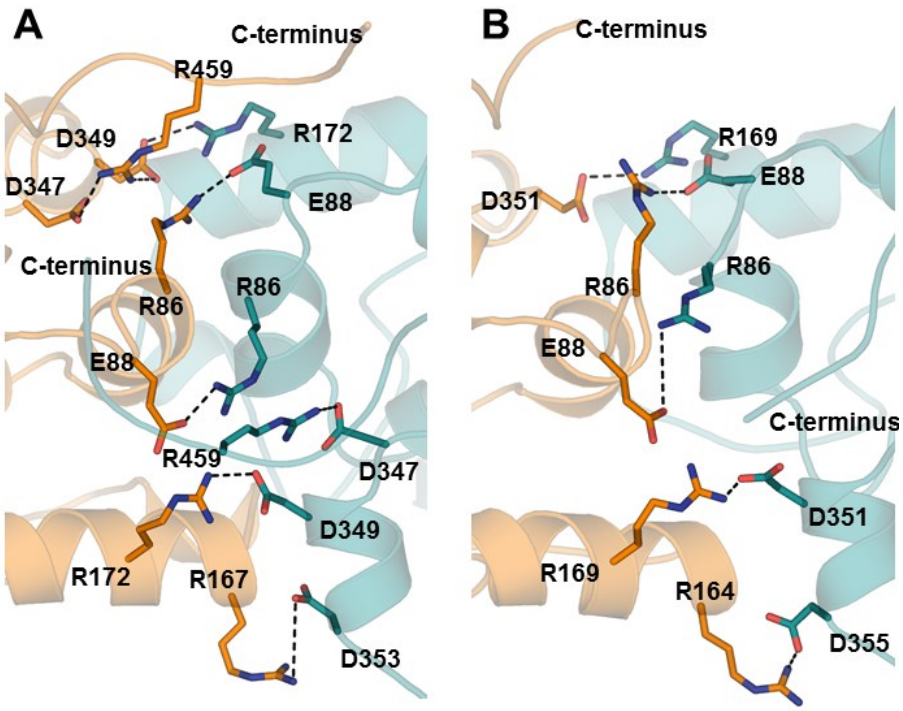

FIG. S1 Both MolA (**A**) and PuhB (**B**) have extensive salt bridge formation across the dimer-dimer interface (orange, blue). The extended length of the MolA C-terminus allows for additional salt-bridge formation *via* R459 (**A**).

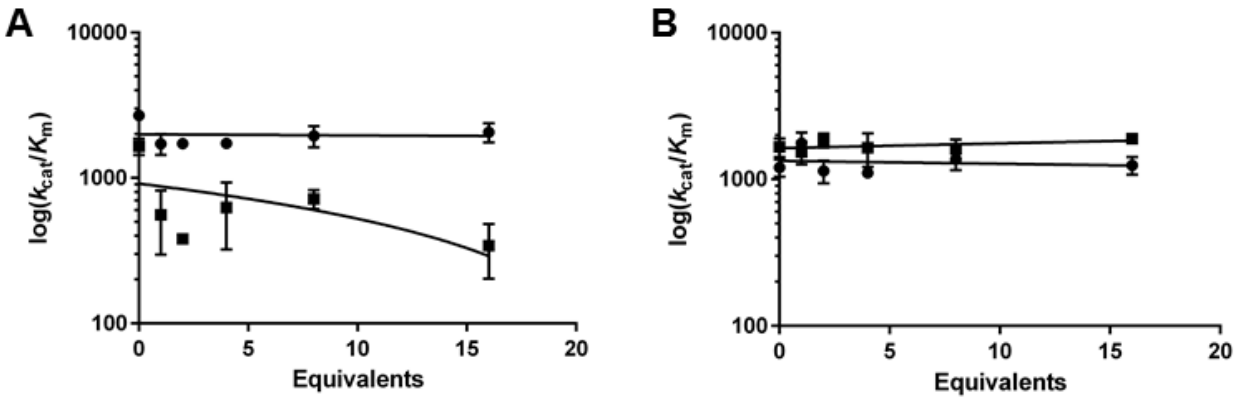

FIG. S2 (**A**) An exogenous supply of cobalt (●) and zinc (■) does not increase the activity of MolA. (**B**) Exogenous bicarbonate addition has no effect on Co-MolA (●) or Zn-MolA (■), in the presence of two equivalents of the respective metals. Error bars represent the standard deviation of two independent replicates. Equivalents refer to the relative concentration of exogenous metal or bicarbonate to protein concentration.

TABLE S1 Effect of the metal cation on molinate hydrolase (MolA) thermostability

Enzyme	Melting point (ºC)
Zinc-MolA	46.0 ± 0.34
Apo-MolA	50.8 ± 0.31

FIGURE S3 (**A**) Substrates from which kinetic parameters could be calculated with molinate hydrolase. (**B**) Substrates with which there was detectable hydrolysis. (**C**) Substrates with which there was no detectable hydrolysis.

A 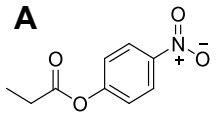 *p*-nitrophenyl propionate	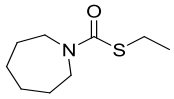 Molinate	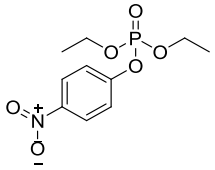 Paraoxon ethyl
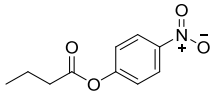 *p*-nitrophenyl butyrate	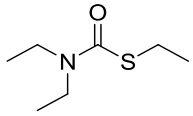 Ethiolate	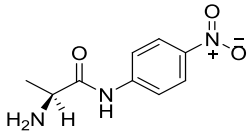 L-alanine *p*-nitroanilide

B 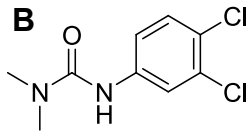 Diuron	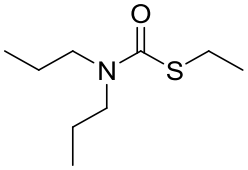 EPTC	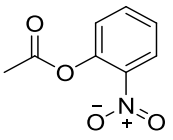 *o*-nitrophenyl acetate
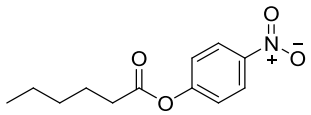 *p*-nitrophenyl hexanoate	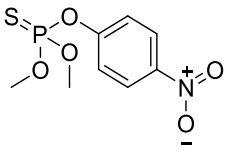 Parathion methyl	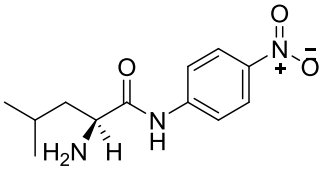 L-leucine *p*-nitroanilide
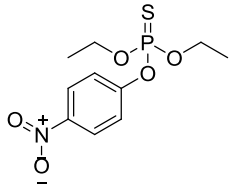 Parathion ethyl	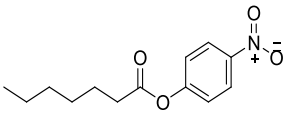 *p*-nitrophenyl octanoate	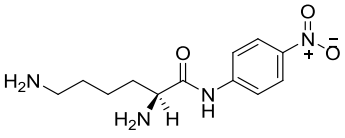 L-lysine *p*-nitroanilide

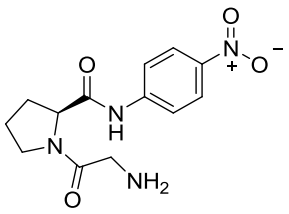

Gly-Pro *p*-nitroanilide

C

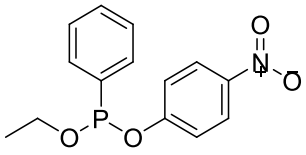

EPN

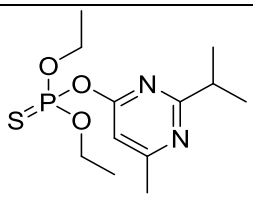

Diazninon

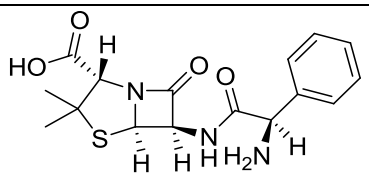

Ampicillin

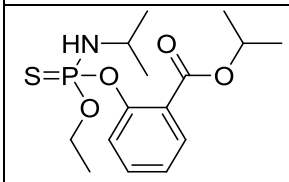

Isofenphos

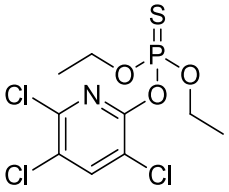

Chlorpyrifos

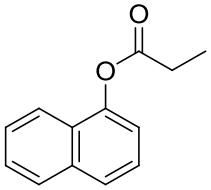

1-Naphthylpropionate

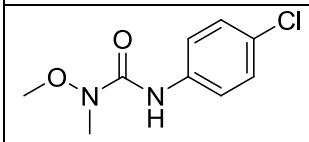

Monolinuron

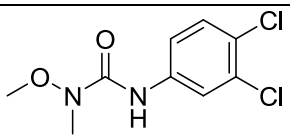

Linuron

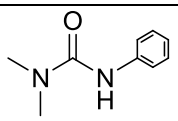

Fenuron

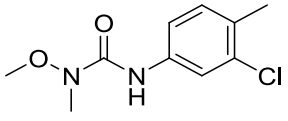

Chlortoluron

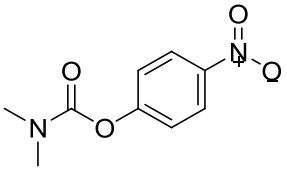

DMNPC

30

TABLE S2 The kinetic parameters for wild-type MolA and variants with molinate, ethiolate, paraoxon ethyl, *p*-nitrophenyl butyrate, L-alanine *p*-nitroanilide and diuron. The k_{cat}/K_m of diuron was estimated using a single fixed substrate concentration well below the K_m. Values shown are the mean and 95% confidence interval of the calculated kinetics.

Substrate	**Variant**	K_m **(μM)**	k_{cat} **(s^{-1})**	k_{cat}/K_m **($M^{-1}s^{-1}$)**
Molinate 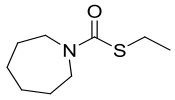	Wild-type	6.88±1.85	$8.24x10^{-3}±6.54x10^{-4}$	$120\ x10^{1}$
	D327E	27.09±1.27	$1.22x10^{-2}±4.62x10^{-4}$	450
	S319G	14.79±4.67	$5.57x10^{-2}±3.21x10^{-3}$	$376\ x\ 10^{1}$
	N69H	0	0	0
	H215N	0	0	0
	F318V	161.27±15.4	$3.29x10^{-3}±1.75x10^{-5}$	20.4
	I73M	17.12±4.54	$1.17x10^{-2}±8.42x10^{-4}$	$153\ x10^{1}$
	V217C	59.42±15.56	$1.17x10^{-2}±2.54x10^{-4}$	197
	F318M	62.17±5.40	$1.16x10^{-2}±3.16x10^{-4}$	189
Ethiolate 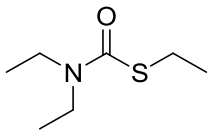	Wild-type	1976.37±322.46	$6.66x10^{-2}±1.79x10^{-3}$	33.7
	D327E	1965.10±722.71	$2.91x10^{-2}±3.31x10^{-3}$	14.8
	S319G	6266.73±1079.17	$6.06x10^{-2}±6.20x10^{-3}$	9.67
	F318V	2914.30±2205.85	$1.03x10^{-2}±2.40x10^{-3}$	3.54
	I73M	6099.57±2524.58	$1.72x10^{-2}±2.93x10^{-3}$	2.81
	V217C	6234.20±286.81	$3.15x10^{-2}±9.23x10^{-4}$	5.05
	F318M	7621.10±3023.30	$2.43x10^{-2}±3.95x10^{-3}$	3.18
	Wild-type	1298.90±132.24	$2.09x10^{-2}±2.32x10^{-3}$	16.1

Paraoxon ethyl 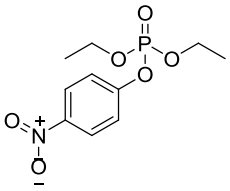	D327E	1756.13±138.53	$4.73x10^{-2}±5.52x10^{-3}$	26.9
	S319G	1591.67±73.84	$6.04x10^{-2}±3.48x10^{-3}$	38.0
	F318V	1965.10±605.32	$2.03x10^{-2}±5.16x10^{-3}$	10.3
	I73M	1930.97±833.69	$1.86x10^{-2}±5.14x10^{-3}$	9.61
	V217C	539.47±88.89	$1.04x10^{-2}±5.43x10^{-4}$	19.3
	F318M	580.65±433.36	$3.72x10^{-3}±2.38x10^{-3}$	6.40
p-Nitrophenyl butyrate 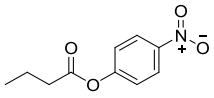	Wild-type	407.20±18.21	$1.37±5.47x10^{-2}$	$336 x10^{1}$
	D327E	400.31±49.65	$1.67±1.02x10^{-1}$	$418 x10^{1}$
	S319G	464.57±28.55	$8.97±2.42x10^{-1}$	$193 x10^{2}$
	F318V	484.63±15.77	$2.28x10^{-1}±5.37x10^{-3}$	470
	I73M	474.67±28.09	$6.49x10^{-1}±1.76x10^{-2}$	$137 x10^{1}$
	V217C	345.06±48.44	$8.28x10^{-1}±5.60x10^{-2}$	$240 x10^{1}$
	F318M	433.24±11.97	$1.15±2.98x10^{-2}$	$266 x10^{1}$
L-Alanine *p*-nitroanilide 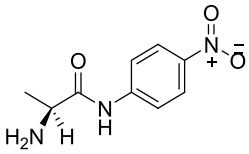	Wild-type	1586.40±605.27	$1.65x10^{-3}±3.21x10^{-4}$	1.04
	D327E	1583.23±331.47	$1.83x10^{-3}±2.22x10^{-4}$	1.15
	S319G	1548.77±258.10	$2.58x10^{-3}±2.33x10^{-4}$	1.67
	F318V	0	0	0
	I73M	816.55±46.60	$1.78x10^{-3}±3.44x10^{-5}$	2.19
	V217C	696.18±18.09	$1.72x10^{-3}±5.69x10^{-5}$	2.47
	F318M	0	0	0
	Wild-type			0.43

Diuron 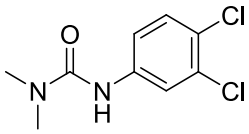	D327E	Could not be determined due to low solubility.	1.67
	S319G		2.43
	F318V		1.20
	I73M		0.28
	V217C		0
	F318M		0.09